

# MEG: Generating Molecular Counterfactual Explanations for Deep Graph Networks

Danilo Numeroso, Davide Bacciu

Department of Computer Science

University of Pisa

Pisa, Italy

danilo.numeroso@phd.unipi.it, bacciu@di.unipi.it

**Abstract**—Explainable AI (XAI) is a research area whose objective is to increase trustworthiness and to enlighten the hidden mechanism of opaque machine learning techniques. This becomes increasingly important in case such models are applied to the chemistry domain, for its potential impact on humans' health, e.g. toxicity analysis in pharmacology. In this paper, we present a novel approach to tackle explainability of deep graph networks in the context of molecule property prediction tasks, named MEG (Molecular Explanation Generator). We generate informative counterfactual explanations for a specific prediction under the form of (valid) compounds with high structural similarity and different predicted properties. Given a trained DGN, we train a reinforcement learning based generator to output counterfactual explanations. At each step, MEG feeds the current candidate counterfactual into the DGN, collects the prediction and uses it to reward the RL agent to guide the exploration. Furthermore, we restrict the action space of the agent in order to only keep actions that maintain the molecule in a valid state. We discuss the results showing how the model can convey non-ML experts with key insights into the learning model focus in the neighbourhood of a molecule.

## I. INTRODUCTION

The ever-growing predictive capabilities of deep learning models have come at the price of increasing complexity in such models. This contributes to the lack of accountability and transparency of the decision-making which intrinsically functions as a black-box. Explainability of AI predictions is extremely important, especially in AI applied to life sciences and their impact on human lives and health [1]. Chemistry is the life science that has seen a surge of related work in the deep learning field, covering health-related tasks such as drug-design, drug-discovery, toxicological analysis and molecule-property prediction in general. The application of deep neural networks in predicting functional and structural properties of chemical compounds is a research topic with long-standing roots [2]. Deep Graph Networks (DGNs) [3], [4] have presently arisen as state-of-the-art for learning effective vectorial molecule representations. As DGNs become able to solve increasingly complex tasks [5], the need of reliable explainability models emerges. The scarce intelligibility of such models and of the internal representation they develop can, in fact, act as a show-stopper for their consolidation, e.g. to predict safety-critical molecule properties, especially when

considering well known issues of opacity in DGN assessment [6].

We present and discuss the most relevant methods regarding explainable deep learning and explainability for graphs in section II.

This paper fits into this latter pioneering field of research by taking a novel angle to the problem, targeting the generation of interpretable counterfactual explanations for the primary use of the experts of the molecular domain. While some work on the generation of human-readable explanations through neural networks does exist [7], [8] and has been introduced in the context of DGNs [9], to the best of our knowledge there exists no prior work targeting counterfactual explanations for graphs.

Hence, we propose MEG (Molecular Counterfactual Generator), a model-agnostic method based on a reinforcement learning [10] explanatory agent. We build our approach upon the assumption that a domain expert would be interested in understanding the model prediction for a specific molecule based on differential case-based reasoning against counterfactuals, i.e. similar structures which the model being explained considers radically different with respect to the predicted property. Such counterfactual molecules should allow the expert to understand if the structure-to-function mapping learnt by the model is coherent with the consolidated domain knowledge, at least for what pertains a tight neighbourhood around the molecule under study. Our approach is specifically thought for molecular applications and the RL agent leverages domain knowledge to constrain the generated explanations to be valid molecules.

We validate our approach on DGNs tackling the prediction of different molecule property prediction tasks, namely binary classification on molecule toxicity and regression on solubility of chemical compounds. First, we run a model selection to pick the best performing model on an held-out validation set. Then, we feed the selected DGN with molecules sampled from an external test set and run a qualitative analysis on its predictions to assess the model behaviour in a plausible operative scenario.

## II. RELATED WORK

### A. Deep Graph Networks

Starting with their introduction by Micheli [11], deep graph networks have rapidly become the state-of-the-art in graph-based tasks. Deep Graph Networks are an evolution of the

classical deep neural networks that are able to work and learn patterns directly from graphs. In graph theory, a graph is defined as a pair  $G = (V, E)$  where  $V$  is a set of entities (nodes) composing the graph and  $E \subseteq V \times V$  represents the relations, i.e. link between nodes, called edges. As far as DGNs are concerned, the plain definition is enriched with node and edge features that are stored in the node-feature matrix  $X \in \mathbb{R}^{n \times d_v}$  and edge-feature matrix  $A \in \mathbb{R}^{m \times d_e}$ , respectively. Therefore, DGNs perform operations on graphs  $G = (V, E, X, A)$ .

DGNs learn by computing information for each node and diffusing it across all the graph. This mechanism is known as context diffusion. At each step, DGNs aggregate information from the node and its neighbours and use it to update the node representation. In general, DGN models can differ on how the context diffusion mechanism is implemented in practice [12]–[14]. In its general form, the neighbourhood aggregation follows a 2-step message passing algorithm: (i) each node in the graph computes a message as a function of its current state  $\mathbf{h}_v^\ell$  and (possibly) edge information. Then, the message is sent to all the neighbours; (ii) each node computes its next state  $\mathbf{h}_v^{\ell+1}$  by aggregating the messages that come from its neighbours. Formally, the neighbourhood aggregation process can be formalised as:

$$\mathbf{h}_v^{\ell+1} = \phi^{\ell+1}(\mathbf{h}_v^{\ell+1}, \Psi(\{\psi^{\ell+1}(\mathbf{h}_u^\ell) \mid u \in \mathcal{N}_v\})) \quad (1)$$

where  $\phi$  and  $\psi$  are transformations of the input data and  $\mathcal{N}_v$  represents the neighbourhood of node  $v$ .  $\Psi$  is a permutation invariant function, e.g. sum, which is required to discard the effect of arbitrary ordering of the set of neighbours. In other words, the output is not influenced by the order in which we evaluate and aggregate neighbours messages.  $\mathbf{h}_v^\ell$  represents the node state (or node representation) at layer  $\ell$ . For  $\ell = 0$ , each node  $v$  is initialised with the associated feature vector  $x_v \in X$ , i.e.  $\mathbf{h}_v^0 = x_v$ .

## B. Explainable AI

The explainability of AI systems is a research topic that aims to explain why and how black-box models, e.g. neural networks, arrive at a specific decision. In general, explainability approaches can be distinguished in *global vs local*. Briefly, a global explanation method aims to provide insights into the model behaviour as a whole, which is usually difficult to obtain as it requires to find a concise description of the model that can be used to predict the future behaviour as well. Conversely, a local explainer relaxes this assumption by explaining how the model behaves for a specific sample (or a sufficiently wide neighbourhood of the input). Any explainability method can be further categorised as *model-specific* or *model-agnostic*, based on whether the method can explain only certain model architectures, i.e. the former, or any model by treating it as a black-box, i.e. the latter.

The most advanced area within this field of research regards the explainability for images and vectorial data. One class of methods are based on sensitivity analysis and falls into the local model-specific category. Symonian, Vedaldi and

Zisserman [15] targets the explanation for an image  $I$  of class  $c$  in Convolutional Neural Networks (CNNs) by taking the derivative of the class score function  $S$  with respect to the input image  $\frac{\delta S}{\delta I}$ . This derivative is then used to build a saliency map indicating the importance of each input feature, i.e. pixels. CAM [16] is an extension of the previous method that aims at finding class-specific feature maps in the latent space, by taking the previous derivative with respect to the penultimate layer of the CNNs. In CAM, the penultimate layer is forced to be convolutional, making the whole method model-specific. LIME [17] takes a different approach, tackling the explanations of complex models by approximating them locally with simpler interpretable models. Such models approximate complex models in a tight locality of a given input  $x_0$ , obtained by perturbing  $x_0$ . As LIME makes no assumptions on the architecture of the model being explained, it falls into the category of model-agnostic methods.

Other approaches within the input perturbation methods include counterfactual explanations. A counterfactual explanation is defined as, starting from a given input, a small perturbation of the starting input configuration which produces a desired prediction (possibly radically different). Furthermore, a good counterfactual must confuse the network being explained while aligning with the underlying data distribution. In other words, it should not present an unlike configuration of features which can easily fool the model. Finding counterfactual explanations can then be defined as an optimisation problem [18]. Van Looveren and Klaise [19] apply counterfactual discovery in classification tasks by using class prototype to align the produced counterfactuals to the data distribution. Different ways to produce counterfactuals include an adversarial term in the objective function [8].

Explainability in the field of deep learning for graphs is, however, much less explored. Although some early-stage effort has been made to generalise established explainability techniques to DGNs [20], [21], these methods turned out to not be as effective in the graph scenario. In this respect, attention must be concentrated towards the development of interpretability techniques specifically tailored to DGNs. While some DGN shows potential for interpretability *by-design* thanks to its probabilistic formulation [14], the majority of works in literature take a neural-based approach which requires the use of an *external* model explainer. GNNE explainer [22] is the front-runner of the model-agnostic methods providing local explanations to neural DGNs in terms of the sub-graph and node features of the input structure which maximally contribute to the prediction. RelEx [23] extends GNNE explainer to surpass the need of accessing the model gradient to learn explanations. GraphLIME [24] attempts to create locally interpretable models for node-level predictions, with application limited to single network data. CoGE [25] introduced contrastive explanations restricted to graph classification problems. Specifically, given a graph along with its prediction, CoGE partitions the training data into the set of graphs having the same label as of the input graph and those with different labels. Thus, it selects a number of graphs from the two sets that are most similar

to the input graph and optimize the Optimal Transport (OT) [26] to obtain the nodes (and edges) that are responsible for the prediction. Finally, as far as life sciences are concerned, the current literature seems lacking in interpretability methods specifically thought for this field. CellBox [27] is one of the few works on the topic. The authors couple the application of a machine learning framework with explicit mathematical models for modeling cellular response to perturbation. The aim is to learn the interactions between cellular components in a supervised setting, combining the learnt features with an ODE solver to enhance the interpretability of the whole model. Therefore, this work aims to achieve interpretability by-design rather than requiring the use of an external explainer. More in general, some of the general interpretability approaches can find room for application in life sciences too [28].

### III. MOLECULAR EXPLANATION GENERATOR (MEG)

#### A. Method Description

The overall architecture of MEG is presented in Fig. 1. We aim to explain the depicted DGN  $\varphi : \mathcal{I} \rightarrow \mathcal{Y}$  that is fit to solve a molecule property prediction task.  $\mathcal{I}$  represents the space of (labelled) molecule structures and  $\mathcal{Y}$  is the task-dependent output space. We assume the DGN to: (i) build vectorial graph representations out of the graph topology and associated information; (ii) grant access to these internal representations.

The explainer  $g$  takes care of generating counterfactual explanations under the form of molecular graphs. The problem of learning to generate generic graph structures is a complex one [29], although some effective solutions exist that are specialized on molecule generation [30]. The generative task tackled by the explainer is, luckily, less general and it is well suited to be implemented by a reinforcement learning based approach. Intuitively, given the sample  $m$ , the explainer  $g$  is trained to identify minimal modifications to  $m$  that maximally change the outcome of the model prediction, obtaining eventually the counterfactual  $m'$  in the figure. Through these changes, one may evaluate the model robustness when it comes to predicting out-of-distribution inputs or finding out critical difficulties, guaranteeing a more thorough understanding of the predictive model itself. In graph structured data, counterfactuals can be obtained by either perturbing the node (or edge) features or the graph topology. The former boils down to perturbation of one-dimensional feature vectors, which is a problem that has been widely explored in the literature and relate to the explainability in a non-relational case [17]. Thus, in this work we focus on finding explanations for a DGN prediction by exclusively alter the graph structure. MEG directly operates on the input molecule topology by means of discrete graph alteration steps.

Molecular counterfactuals ought to satisfy three properties: (i) they need to resemble the molecule under study; (ii) predicted properties on counterfactuals must differ substantially from those predicted on the input one; (iii) molecular counterfactuals need to be in compliance with chemical constraints. To this end, the agent  $g$  receives information about an input molecule  $m$  and its associated prediction score  $\varphi(m)$ ,

and generates a molecular counterfactual  $m'$ , leveraging prior domain knowledge to ensure validity of the generated sample. Counterfactual generation is formalised as a maximisation problem in which, given a target molecule  $m$  with prediction  $\varphi(m)$ , the generator  $g$  is trained to optimize:

$$\arg \max_{\theta} \mathcal{L}(\varphi(m), (\varphi \circ g)(\cdot | \theta)) + \mathcal{K}[m, g(\cdot | \theta)]. \quad (2)$$

Where  $\theta$  indicates the explainer learnt parameters. The composition  $(\varphi \circ g)(\cdot | \theta)$  formalizes the model  $\varphi$  counter-predictions, made over the counterfactuals produced by  $g$ . Given the counterfactual  $m' = g(\cdot | \theta)$  we rewrite (2) as

$$\arg \max_{m'} \mathcal{L}(\varphi(m), \varphi(m')) + \mathcal{K}[m, m'] \quad (3)$$

where  $\mathcal{L}$  is a measure of dissimilarity between the model predictions for the molecule  $m$  and its counterfactual  $m'$ , while  $\mathcal{K}$  measures the structural similarity between the molecules  $(m, m')$  themselves. Note that the  $\arg \max$  operator is applied on both  $\mathcal{L}$  and  $\mathcal{K}$  so that the generator can optimise the two properties jointly.

The main use of counterfactual explanations is to provide insights into the function learnt by the model  $\varphi$ . In this sense, a set of counterfactuals for a molecule may be used to: (i) identify changes to the molecular structure leading to substantial changes in the properties, enabling domain experts to discriminate whether the model predictions are well founded; (ii) validate existing interpretability approaches, by running them on both the original input graph and its related counterfactual explanations. The main idea behind this latter point is that a local interpretation method may provide explanations that work well within a very narrow range of the input, but do not give a strong suggestion on a wider behaviour. To show evidence and usefulness of such a differential analysis, in section IV we use our counterfactuals to assess the quality of explanations given by GNNExplainer [22]. Given the undirected nature of the graphs in our molecular application, we restrict the original GNNExplainer model to discard the effect of edge orientation on the explanation.

#### B. Explanation Generator

The explanation generator  $g$  has access to the internal representation of the property-prediction model as well as to its output and uses this information to guide the exploration of the molecular structure space to seek for the nearest counterfactuals. Given the non-differentiable nature of the graph alterations and its ease in modelling and handling multi-objective optimization, we model  $g$  through a multi-objective RL problem [31]. This allows to easily steer towards the generation of counterfactuals optimizing several properties at a time [32], [33].

Formally, the problem takes the form of a Markov Decision Process (MDP)  $(\mathcal{S}, \mathcal{A}, \mathcal{Q}, \pi, \mathcal{R}, \gamma)$ . The set of states  $\mathcal{S}$  includes all the possible molecules that can be generated by MEG. In our framework,  $m$  is used to bootstrap the generative process in  $g$ , i.e.  $s_0 = m$  which operates on the current candidate

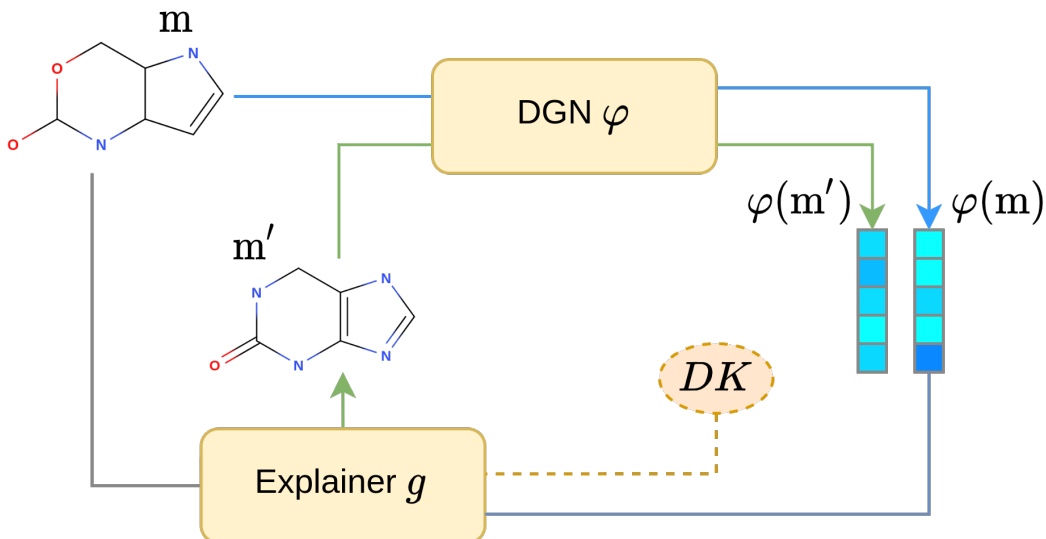


Fig. 1: Architecture of the Molecular Explanation Generator (MEG): DGN  $\varphi$  is a trained molecule property predictor, whereas the Explainer  $g$  is a generative agent producing counterfactuals, constrained by prior domain knowledge  $DK$ .

counterfactual with graph editing operations under domain knowledge constraints.

The action space  $\mathcal{A}$  requires particular attention to ensure that all the generated counterfactuals complies to natural chemical rules. Thus, domain knowledge must be imbued into  $\mathcal{A}$ . To achieve validity of the counterfactuals, we base the implementation of the generator on the MolDQN [34] model. The key element is that we borrow the structure of the action space, in which given the current state  $s_t$ , we obtain  $\mathcal{A}_t$  as union of three different sets of actions:

- $\mathcal{A}_a$ , made up of all possible atom additions. First, we add a new atom  $v$  to the atom sets, i.e,  $V' = V \cup \{v\}$  and then bind it to an atom  $u \in V$ . If the resulting molecule does not violate any chemical constraints, the action is retained. Otherwise it is discarded.
- $\mathcal{A}_b^+$ , representing the set of bond additions. We scan the set of atoms  $V$  pair-wisely and either add a new bond or increase the bond order in case the two current atoms are already linked, as follows:
  - 1) No bond  $\longrightarrow$  {Single, Double, Triple} bond
  - 2) Single bond  $\longrightarrow$  {Double, Triple} bond.
  - 3) Double bond  $\longrightarrow$  {Triple} bond.
- $\mathcal{A}_b^-$ , representing the set of bond removals which is obtained by reversely applying the bond addition rules.

Therefore, they are all combined to construct the action space  $\mathcal{A}_t = \mathcal{A}_a \cup \mathcal{A}_b^+ \cup \mathcal{A}_b^- \cup \{\perp\}$ , where  $\perp$  is a special action indicating to leave the molecule as is. Eventually,  $\mathcal{A}_t$  is constrained to discard actions that would lead the molecule in an invalid state, e.g. violation of valence rules.

The multi-objective reward function  $\mathcal{R}$  exploits the prediction from  $\varphi$  so as to notify the agent of its current performance, emitting a scalar reward. The term  $\gamma$  is called discount and is incorporated into  $\mathcal{R}$  to weight the contribution of distant

future reward signals. In our design,  $\mathcal{R}$  binds together a term regulating the change in prediction scores, which is inherently task-dependent, with a second term controlling similarity between the original molecule and its counterfactual, as presented in (2).

We explored three different formulations for the latter term. First, the Tanimoto similarity over the binary Morgan fingerprints [35]:

$$\mathcal{T}(a, b) = \frac{a \cdot b}{\|a\|^2 + \|b\|^2 - a \cdot b}. \quad (4)$$

As this metric looks for matching molecule fragments, it may be too susceptible to graph alteration actions. To surpass this issue, we alternatively compare the molecule similarity in the DGN latent space. Thus, we leverage the model’s own perception of similarity between molecules by directly comparing the internal vectorial molecule representations through cosine similarity:

$$\cos(m, m') = \frac{\mathbf{h}_m \cdot \mathbf{h}_{m'}}{\|\mathbf{h}_m\| \|\mathbf{h}_{m'}\|}. \quad (5)$$

However, in our empirical settings we found it useful to combine the model perception with a fragment-based metric such as the tanimoto similarity. For this reason, we derive a third similarity metric which is a convex combination of the tanimoto similarity (structural) and the neural encoding similarity (model perception):

$$\mathcal{K}(m, m') = \alpha_1 \mathcal{T}(m, m') + \alpha_2 \cos(m, m') \mid \sum_i \alpha_i = 1. \quad (6)$$

Lastly, given the current state  $s_t$  and a sampled action  $a_t$ , the explainer evaluates the goodness of the pair action-state through the  $Q$  function. Since the state space can become combinatorially large,  $Q$  is approximated by a double deep-Q-network [36] composed of four linear layers. Finally, the

policy  $\pi$  is a function outputting the best possible action given any state  $s \in \mathcal{S}$ . We use either a decaying  $\varepsilon$ -greedy policy or an  $\varepsilon$ -greedy policy to balance exploration and exploitation, depending on whether we are targeting the optimisation of a single counterfactual or a group of them.

### C. Training the Generator

When it comes to training the generator, we must specify the task-dependent term  $\mathcal{L}$  in the reward function (3). First of all, in a multi-objective reward function the reward is returned as a vector of partial scalar rewards  $r_i$ , with one partial reward for each property we are seeking to optimize. An intuitive way to combine all the partial rewards is by convex combination:

$$r^t = \sum_i \alpha_i r_i^t$$

subject to  $\sum_i \alpha_i = 1$ . The choice of the coefficients is treated as a model hyper-parameter.

The task-dependent term  $\mathcal{L}$  in (3) can be specialized for classification and regression tasks. As regards classification, given a set of classes  $\mathcal{C}$ , a model  $\varphi$  emits a probability distribution  $\varphi(\cdot) = \mathbf{y} = [y_0, \dots, y_{|\mathcal{C}|}]$  over the predicted classes. In this case, given an input-prediction pair  $\langle m, c = \arg \max_{c \in \mathcal{C}} \varphi(m) \rangle$ , the generator is trained to produce counterfactual explanations  $m'$  minimising the prediction score for class  $c$ , as follows

$$\arg \max_{m'} -\alpha y_c + (1 - \alpha) \mathcal{K}[m', m] \quad (7)$$

where  $\alpha \in [0, 1]$ . Hence, the model  $\varphi$  returns at each step a smooth reward, which is actually the inverse of the probability of  $m'$  belonging to class  $c$ . Differently, we define the loss objective for a regression task as

$$\arg \max_{m'} \alpha \beta \|s_{m'} - s_m\|_1 + (1 - \alpha) \mathcal{K}[m', m] \quad (8)$$

where  $s$  is the regression target and  $s_m$  and  $s_{m'}$  are the predicted values for the original molecule and its counterfactual, respectively. Lastly,  $\beta = \text{sgn}(\|s_{m'} - s\|_1 - \|s_m - s\|_1)$  prevents the agent from generating molecules whose predicted scores move towards the original target.

## IV. EXPERIMENTAL EVALUATION

### A. Datasets and model configuration

We test MEG on two popular molecule property prediction benchmarks: TOX21 [37], addressing toxicity prediction as a binary classification task, and ESOL [38], that is a regressive task on water solubility of chemical compounds.

Preliminarily, we scanned both datasets to filter non-valid chemical compounds. We considered structures to be valid molecules if they pass the RDKit [39] sanitization check. In the end, TOX21 comprises 1756 samples, equally distributed among the two classes, while ESOL includes 1129 compounds. We choose a split of 80%/10%/10% for training, validation and test set in both datasets.

The trained DGN comprises three GraphConv [40] layers with ReLU activations. The model has been implemented

Dataset	HS	Batch Size	LR	Optimizer	TR	VL
TOX21	256	20	$1 \times 10^{-3}$	Adam	94%	88%
ESOL	32	20	$5 \times 10^{-4}$	Adam	0.31	0.57

TABLE I: HS = hidden size, LR = learning rate, TR = training, VL = validation

Molecule	Target	Prediction	Similarity	Reward
A0: Fig. 2	NoTox	NoTox (0.99)	-	-
A1: Fig. 2	-	Tox (0.99)	0.81	0.86
A2: Fig. 2	-	Tox (0.99)	0.74	0.85
A3: Fig. 2	-	Tox (0.99)	0.74	0.85
B0: Fig. 3	Tox	Tox (0.99)	-	-
B1: Fig. 3	-	NoTox (0.93)	0.77	0.78
B2: Fig. 3	-	NoTox (0.89)	0.74	0.77
C0: Fig. 4	-4.28	-4.01	-	-
C1: Fig. 4	-	-6.11	0.63	1.37
C2: Fig. 4	-	-5.93	0.64	1.23
C3: Fig. 4	-	-5.07	0.63	1.18
D0: Fig. 5	-5.23	-5.31	-	-
D1: Fig. 5	-	-6.95	0.71	1.45
E0: Fig. 5	-1.62	-1.75	-	-
E1: Fig. 5	-	-2.94	0.74	1.18

TABLE II: Summary of results. A0 and B0 refers to molecules belonging to TOX21, whereas C0, D0 and E0 belong to ESOL. Subsequent indexes refer to the related counterfactual explanations.

by using PyTorch Geometric [41] and trained with Adam optimizer.

We ran a model selection and select the model that achieved the highest result on the validation set. We optimized the hyper-parameters by grid-search over the learning rate in  $\{5 \times 10^{-3}, 1 \times 10^{-3}, 5 \times 10^{-4}, 1 \times 10^{-4}\}$ , batch size in  $\{20, 60, 120\}$  and hidden size in  $\{32, 64, 128, 256\}$ . The best configuration for both models is reported in Table I.

The network builds a layer-wise molecular representation via concatenation of max and mean pooling operations, over the set of node representations. The final neural encoding of the molecule is obtained by sum-pooling of the intermediate representations. This neural encoding is then fed to a three-layer feed-forward network, with hidden sizes of [128, 64, 32] and dropout set to 0.1, to perform the final property prediction step. Then, we feed the model with molecules in the test set on which it achieved 77% of accuracy for TOX21 and 0.57 MSE for ESOL, and try to explain the predictions.

During generation, we employed MEG to find 10 counterfactual explanations for each molecule in test, ranked according to the multi-objective score in Section III. In order to comply with the similarity criterion, we set as starting point for the generation the original test molecule and limit the episode length to 1. Furthermore, we remove  $\perp$  from the list of available actions and use a decaying epsilon greedy policy  $\varepsilon_{t+1} = \lambda \varepsilon_t$  with  $\lambda = 0.9987$ . Finally, we train MEG for 3000 epochs.

### B. Explainability Results and Discussion

We present some quantitative results in Table II, listing some of the best counterfactual explanations collected for some samples in both tasks. Both experiments have been tested

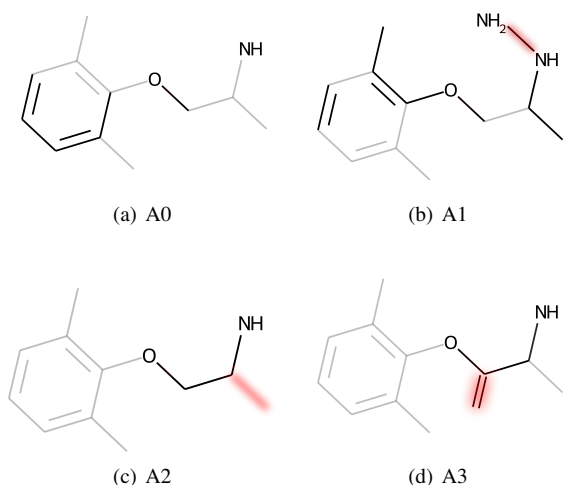


Fig. 2: Counterfactual explanations (A1-3) for a non-toxic molecule (A0).

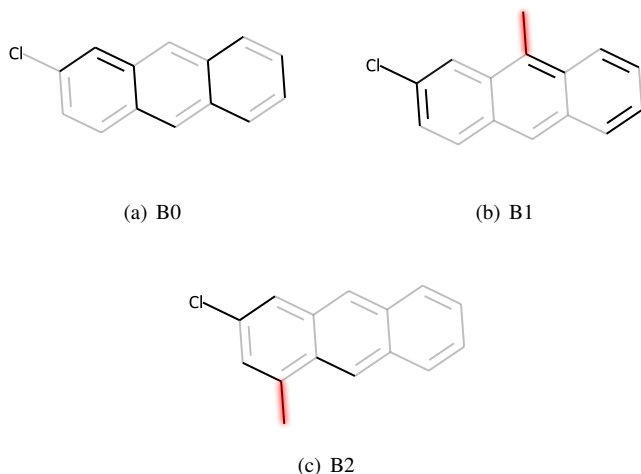


Fig. 3: Toxic molecule (B0) classified as non toxic after the addition of one atom of carbon (B1-2).

with the convex combination between the neural encoding similarity and the Tanimoto, described in (6).

Qualitative results are shown in Fig. 2, Fig. 3, Fig. 4 and Fig. 5. To ease the interpretation of our results, counterfactual modifications have been highlighted in red, while blurred edges represent those edges that have been masked out by GNNExplainer predictions. In other words, GNNExplainer interpretations are the sub-graphs formed by non-blurred edges. By our examples, we:

- highlight some of the qualitative differential reasoning that experts can carry out.
- show that GNNExplainer, by its very nature, generates explanations specifically tied with the input graph, making it difficult to find evidences in the global behaviour of the model. This is true for any model that follows closely

the local explanation paradigm. We argue the necessity to output explanations that maintain their validity in a neighbourhood of the input graph of arbitrary size.

In TOX21, we analyse one representative result for each class of prediction. In A0 (Fig. 2), we take a molecule that has been correctly classified by the DGN as being non-toxic and generate three counterfactuals for it. Similarly, in B0 (Fig. 3) we do the same for a toxic molecule. In both examples, the counterfactuals are classified as the opposite class with respect to the original one, as reported in Table II. In the first place, it is easy for domain experts to run qualitative analyses of the DGN predictions on our counterfactuals. In the first sample, we see three valid modifications of A0, specifically the addition of an atom of nitrogen (A1), the removal of carbon (A2) and the addition of an atom of carbon linked to the molecule through a double bond (A3). In all these cases, it is sufficient to check whether these modifications can move the prediction from non-toxic to toxic also in a real-world scenario. Correspondingly, in the toxic compound case (B0) the molecules resulting from addition of C, i.e B1-B2, are classified as non-toxic. Being able to highlight such behaviours is crucial when predicting safety-critical properties, e.g in drug design.

Focusing on GNNExplainer interpretations, our counterfactuals show some difficulties that any local explainer based on single-instance explanation can encounter. First, we recall that GNNExplainer provides sample-level explanations by masking out low-importance edges in the graph. However, explanations limited to a single instance are difficult to generalise to other unexplained samples. This means that we have no clues on the out-of-instance model behaviour, making it difficult to guess how the model would react to unseen graphs. In fact, we see that in both Fig. 2, Fig. 3 the original explanations (A0-B0) have not identified as important certain substructures that have been eventually modified by our counterfactuals to change the prediction.

We now turn the attention to ESOL results, i.e C0-D0-E0 shown in Table II. C0 (Fig. 4) is a well-known organic compound named pentachlorophenol, commonly used as a pesticide or a disinfectant, and is characterised by nearly absolute insolubility in water. While the DGN achieved good predictive performance for its aqueous solubility value, the counterfactuals underlined that the models predicts less solubility in case the oxygen atom is removed (e.g, C2), or modified somehow (e.g, C1, C3), highlighting how it is highly relevant for the DGN prediction. As in the TOX21 samples, such relation is not adequately captured by GNNExplainer.

In the last sample, we bring a purely qualitative analysis of two molecules (Fig. 5). In D0, we have a molecule of phosalone, while E0 is a molecule of thiofanox. MEG derives the two associated counterfactuals D1-E1 by performing complementary actions. In the first case, MEG finds D1 by removing an atom of sulphur from D0 while E1 is obtained by the addition of sulphur to E0. In both cases, though, the model prediction outputs lower values of solubility with respect to the original inputs (see Table II). If the addition of sulphur makes

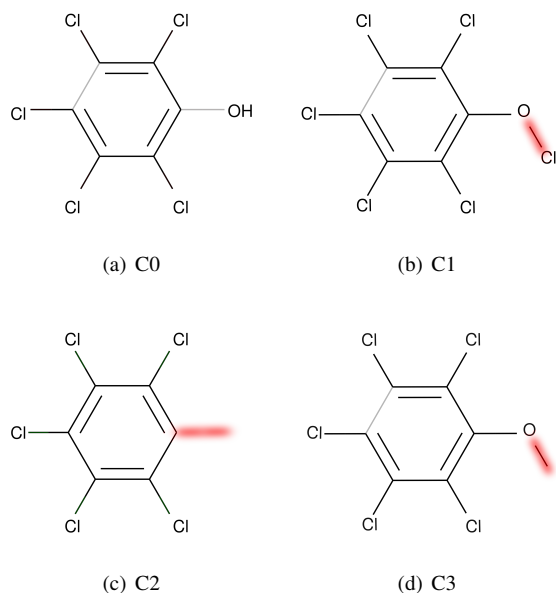


Fig. 4: ESOL sample alongside its counterfactuals (C1-3). Quantitative results are reported in Table II.

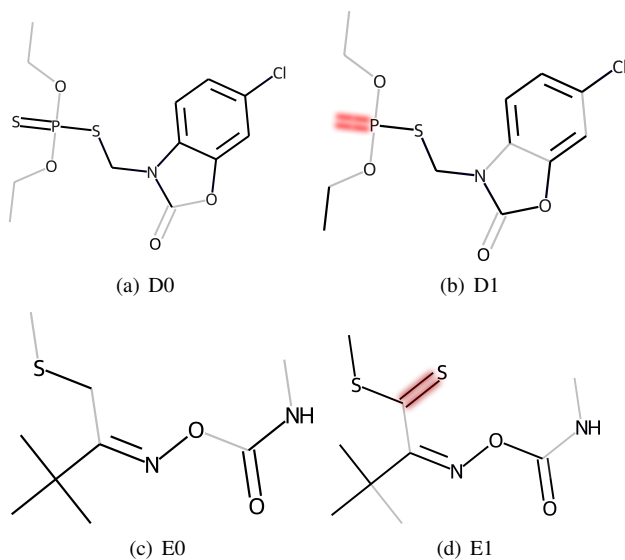


Fig. 5: First row: MEG removes sulphur, DGN solubility prediction decreases (Table II). Second row: MEG adds sulphur, DGN predicts less solubility nonetheless.

the water solubility of a compound to decrease, the prediction of E1 is not faithful. Vice versa, if sulphur increases the water solubility,  $\varphi(D1)$  is not reliable. Although  $\varphi(D0)$  and  $\varphi(E0)$  are precise with respect to the ground truth values, such an analysis shows indications that the learnt function may not be trustworthy. It is our hope that, based on our interpretability approach, an expert of the molecular domain could be able to gain a better insight into the whether the properties and patterns captured by the predictive model are meaningful from

a chemical standpoint.

## V. CONCLUSIONS

We have presented MEG, a novel interpretability framework that tackles explainability in the chemical domain by generation of molecular counterfactual explanations. MEG can work with any DGN model as we only exploit input-output properties of such models.

We show As a general comment of the results, one can note that while a local approach such as GNNExplainer may give good approximations when it comes to explaining the specific prediction, it lacks sufficient breadth to characterize the model behaviour already in a near vicinity of the sample under consideration. On the other hand, our counterfactual interpretation approach may find new samples which are likely to highlight the causes of a given model prediction, providing a better approximation to a locally interpretable model, e.g. C1-3 in Fig. 4. Furthermore, MEG can help to detect some critical issues on toxicity prediction of a given model, e.g. B1-2 (Fig. 3), that may affect humans' health if employed in the drug design setting. In conclusion, apart for its value in generating explanations that are well understood by a domain expert, MEG can work both as a sanity checker for other local model explainers, as well as a sampling method to strengthen the coverage and validity of local interpretable explanations, such as in the original LIME method for vectorial data [17].

## ACKNOWLEDGEMENT

The work is supported by project MIUR-SIR 2014 LIST-IT (grant n. RBSI14STDE) and by TAILOR, a project funded by EU Horizon 2020 research and innovation programme under GA No 952215.

## REFERENCES

- [1] Davide Bacciu, Battista Biggio, Paulo Lisboa, José D. Martín, Luca Oneto, and Alfredo Vellido. Societal issues in machine learning: When learning from data is not enough. In *27th European Symposium on Artificial Neural Networks, ESANN 2019, Bruges, Belgium, April 24-26, 2019*, 2019.
- [2] Alessio Micheli, Alessandro Sperduti, and Antonina Starita. An introduction to recursive neural networks and kernel methods for cheminformatics. *Current Pharmaceutical Design*, 13(8), 2007.
- [3] Jie Zhou, Ganqu Cui, Zhengyan Zhang, Cheng Yang, Zhiyuan Liu, Lifeng Wang, Changcheng Li, and Maosong Sun. Graph neural networks: A review of methods and applications, 2018.
- [4] Davide Bacciu, Federico Errica, Alessio Micheli, and Marco Podda. A gentle introduction to deep learning for graphs. *Neural Networks*, 129:203–221, 2020.
- [5] Justin Gilmer, Samuel S. Schoenholz, Patrick F. Riley, Oriol Vinyals, and George E. Dahl. Neural message passing for quantum chemistry. volume 70 of *Proceedings of Machine Learning Research*, pages 1263–1272, International Convention Centre, Sydney, Australia, 06–11 Aug 2017. PMLR.
- [6] Federico Errica, Marco Podda, Davide Bacciu, and Alessio Micheli. A fair comparison of graph neural networks for graph classification. In *International Conference on Learning Representations*, 2020.
- [7] A. Agrawal, J. Lu, S. Antol, M. Mitchell, C. Lawrence Zitnick, D. Batra, and D. Parikh. Vqa: Visual question answering, 2015.
- [8] Yunxia Zhao. Fast real-time counterfactual explanations, 2020.
- [9] Hao Yuan, Jiliang Tang, Xia Hu, and Shuiwang Ji. Xggn: Towards model-level explanations of graph neural networks. *Proceedings of the 26th ACM SIGKDD International Conference on Knowledge Discovery & Data Mining*, Jul 2020.

- [10] Richard S Sutton and Andrew G Barto. Reinforcement learning: an introduction cambridge. MA: MIT Press.[Google Scholar], 1998.
- [11] A. Micheli. Neural network for graphs: A contextual constructive approach. *IEEE Transactions on Neural Networks*, 20(3):498–511, 2009.
- [12] Thomas N. Kipf and Max Welling. Semi-supervised classification with graph convolutional networks, 2017.
- [13] William L. Hamilton, Rex Ying, and Jure Leskovec. Inductive representation learning on large graphs. In *NIPS*, 2017.
- [14] Davide Bacciu, Federico Errica, and Alessio Micheli. Probabilistic learning on graphs via contextual architectures. *Journal of Machine Learning Research*, 21(134):1–39, 2020.
- [15] Karen Simonyan, Andrea Vedaldi, and Andrew Zisserman. Deep inside convolutional networks: Visualising image classification models and saliency maps, 2013.
- [16] Bolei Zhou, Aditya Khosla, Agata Lapedriza, Aude Oliva, and Antonio Torralba. Learning deep features for discriminative localization, 2015.
- [17] Marco Tulio Ribeiro, Sameer Singh, and Carlos Guestrin. "why should I trust you?": Explaining the predictions of any classifier. In *Proceedings of the 22nd ACM SIGKDD International Conference on Knowledge Discovery and Data Mining, San Francisco, CA, USA, August 13-17, 2016*, pages 1135–1144, 2016.
- [18] Sandra Wachter, Brent Mittelstadt, and Chris Russell. Counterfactual explanations without opening the black box: Automated decisions and the gdpr, 2018.
- [19] Arnaud Van Looveren and Janis Klaise. Interpretable counterfactual explanations guided by prototypes, 2020.
- [20] Federico Baldassarre and Hossein Azizpour. Explainability techniques for graph convolutional networks. *arXiv preprint arXiv:1905.13686*, 2019.
- [21] Phillip E Pope, Soheil Kolouri, Mohammad Rostami, Charles E Martin, and Heiko Hoffmann. Explainability methods for graph convolutional neural networks. In *Proceedings of the IEEE Conference on Computer Vision and Pattern Recognition*, pages 10772–10781, 2019.
- [22] Rex Ying, Dylan Bourgeois, Jiaxuan You, Marinka Zitnik, and Jure Leskovec. Gnnexplainer: Generating explanations for graph neural networks, 2019.
- [23] Yue Zhang, David Defazio, and Arti Ramesh. Relex: A model-agnostic relational model explainer, 2020.
- [24] Qiang Huang, Makoto Yamada, Yuan Tian, Dinesh Singh, Dawei Yin, and Yi Chang. Graphlime: Local interpretable model explanations for graph neural networks, 2020.
- [25] Lukas Faber, Amin K. Moghaddam, and Roger Wattenhofer. Contrastive graph neural network explanation, 2020.
- [26] Giannis Nikolentzos, Polykarpos Meladianos, and Michalis Vazirgiannis. Matching node embeddings for graph similarity. In *Proceedings of the AAAI Conference on Artificial Intelligence*, volume 31, 2017.
- [27] Bo Yuan, Ciyue Shen, Augustin Luna, Anil Korkut, Debora S Marks, John Ingraham, and Chris Sander. Interpretable machine learning for perturbation biology. *bioRxiv*, page 746842, 2020.
- [28] Christina B. Azodi, Jiliang Tang, and Shin-Han Shiu. Opening the black box: Interpretable machine learning for geneticists. *Trends in Genetics*, 36(6):442 – 455, 2020.
- [29] Davide Bacciu, Alessio Micheli, and Marco Podda. Edge-based sequential graph generation with recurrent neural networks. *Neurocomputing*, 416:177 – 189, 2020.
- [30] Marco Podda, Davide Bacciu, and Alessio Micheli. A deep generative model for fragment-based molecule generation. In Silvia Chiappa and Roberto Calandra, editors, *The 23rd International Conference on Artificial Intelligence and Statistics, AISTATS 2020, 26-28 August 2020, Online [Palermo, Sicily, Italy]*, volume 108 of *Proceedings of Machine Learning Research*, pages 2240–2250. PMLR, 2020.
- [31] C. Liu, X. Xu, and D. Hu. Multiobjective reinforcement learning: A comprehensive overview. *IEEE Transactions on Systems, Man, and Cybernetics: Systems*, 45(3):385–398, 2015.
- [32] Benjamin Sanchez-Lengeling, Carlos Outeiral, Gabriel L. Guimaraes, and Alan Aspuru-Guzik. Optimizing distributions over molecular space. an objective-reinforced generative adversarial network for inverse-design chemistry (organic), Aug 2017.
- [33] Mariya Popova, Olexandr Isayev, and Alexander Tropsha. Deep reinforcement learning for de novo drug design. *Science Advances*, 4(7):eaap7885, Jul 2018.
- [34] Zhenpeng Zhou, Steven Kearnes, Li Li, Richard N. Zare, and Patrick Riley. Optimization of molecules via deep reinforcement learning, 2018.
- [35] David Rogers and Mathew Hahn. Extended-connectivity fingerprints. *Journal of Chemical Information and Modeling*, 50(5):742–754, 2010. PMID: 20426451.
- [36] Hado van Hasselt, Arthur Guez, and David Silver. Deep reinforcement learning with double q-learning, 2015.
- [37] Kristian Kersting, Nils M. Kriege, Christopher Morris, Petra Mutzel, and Marion Neumann. Benchmark data sets for graph kernels, 2016.
- [38] Zhenqin Wu, Bharath Ramsundar, Evan N. Feinberg, Joseph Gomes, Caleb Geniesse, Aneesh S. Pappu, Karl Leswing, and Vijay Pande. Moleculenet: A benchmark for molecular machine learning, 2017.
- [39] Greg Landrum et al. Rdkit: Open-source cheminformatics, 2006.
- [40] Christopher Morris, Martin Ritzert, Matthias Fey, William L. Hamilton, Jan Eric Lenssen, Gaurav Rattan, and Martin Grohe. Weisfeiler and leman go neural: Higher-order graph neural networks, 2018.
- [41] Matthias Fey and Jan E. Lenssen. Fast graph representation learning with PyTorch Geometric. In *ICLR Workshop on Representation Learning on Graphs and Manifolds*, 2019.